

# HADRON DIFFRACTIVE SCATTERING AT ULTRAHIGH ENERGIES AND COULOMB INTERACTION

V.V. ANISOVICH and V.A. NIKONOV

*National Research Centre "Kurchatov Institute", Petersburg Nuclear Physics Institute, Gatchina  
188300, Russia*

Received Day Month Year  
Revised Day Month Year

We study the interplay of hadronic and Coulomb interactions for  $pp$  scattering at LHC energies on the basis of the previous determination of the real part of the amplitude [V.V. Anisovich, V.A. Nikonov, J. Nyiri, Int. J. Mod. Phys. A **30**, 1550188 (2015)]. The interference of hadron and Coulomb interactions is discussed in terms of the  $K$ -matrix function technique. Supposing the black disk mode for the asymptotic interaction of hadrons, we calculate interference effects for the energies right up to  $\sqrt{s} = 10^6$  TeV. It turns out that the real part of the amplitude is concentrated in the impact parameter space at the border of the black disk that results in a growth of interplay effects with the energy increase.

PACS numbers: 13.85.Lg, 13.85.-t, 13.75.Cs, 14.20.Dh

## 1. Introduction

At energies of LHC<sup>1-4</sup> the profile function of the  $pp$ -scattering amplitude,  $T(b)$ , reaches the black disk limit at small  $b$ . The black disk picture corresponds to the non-coherent parton interactions in hadron collisions. For the black disk scenario the profile function at  $\sqrt{s} \gtrsim 100$  TeV gets frozen inside the disk area,  $T(b) \simeq 1$  at  $b < R_{black\ disk}$ , and the increasing radius of the black disk,  $R_{black\ disk}$ , determines the total, elastic and inelastic cross sections:  $\sigma_{tot} \simeq 2\pi R_{black\ disk}^2$ ,  $\sigma_{el} \simeq \pi R_{black\ disk}^2$  and  $\sigma_{inel} \simeq \pi R_{black\ disk}^2$ .

Hadron physics at ultrahigh energies is a physics of large energy logarithms,  $\ln s \equiv \xi \gg 1$ ,<sup>5-9</sup> and increasing parton disks.<sup>10-12</sup> Considering an interplay of hadron and Coulomb interactions in this energy region we concentrate our attention on the black disk mode.

Using notations of ref.<sup>12</sup> we present the hadronic scattering amplitude with switched off Coulomb interaction as follows:

$$A(\mathbf{q}^2, \xi) = \int d^2b e^{i\mathbf{q}\mathbf{b}} T(b, \xi), \quad (1)$$

$$T(b, \xi) = 1 - \eta(b, \xi) \exp(2i\delta(b, \xi)) = \frac{-2iK(b, \xi)}{1 - iK(b, \xi)},$$

where  $\xi = \ln s$ ,  $b = |\mathbf{b}|$ . For the profile function we write:

$$T(b, \xi) = T_{\Im}(b, \xi) - iT_{\Re}(b, \xi), \quad T_{\Re}(b, \ln s) \simeq \frac{\pi}{2} \frac{\partial T_{\Im}(b, \ln s)}{\partial(\ln s)}. \quad (2)$$

At the asymptotic regime the imaginary part of the amplitude is a generating function for  $A_{\Re}(\mathbf{q}^2, \ln s)$  that is based on asymptotic equality  $[\sigma_{tot}(pp)/\sigma_{tot}(p\bar{p})]_{\sqrt{s} \rightarrow \infty} = 1$  (see<sup>12</sup> for detail). The total and diffractive cross sections read:

$$\sigma_{tot} = 2 \int d^2b T_{\Im}(b, \xi), \quad 4\pi \frac{d\sigma_{el}}{d\mathbf{q}^2} = (1 + \rho^2) A_{\Im}^2(\mathbf{q}^2), \quad (3)$$

with the usual notation  $A_{\Re}^H(\mathbf{q}^2, \xi)/A_{\Im}^H(\mathbf{q}^2, \xi) = \rho(\mathbf{q}^2, \xi)$ . Taking into account that  $\rho^2$  is small,  $\rho^2 \sim 0.01$ , one can approximate:

$$|A_{\Im}(\mathbf{q}^2, \xi)| \simeq 2\pi^{\frac{1}{2}} \sqrt{\frac{d\sigma_{el}}{d\mathbf{q}^2}}, \quad (4)$$

that makes direct calculations of the real part of the scattering amplitude,  $A_{\Re}(\mathbf{q}^2, \xi)$ , possible, basing on the energy dependence of the diffractive scattering cross section. The corresponding calculations were performed in ref.<sup>12,13</sup> using the data at  $\sqrt{s} \sim 5 - 50 \text{ TeV}^{1-4}$  and the results of the previous analyses.<sup>9-11</sup> In ref.<sup>12,13</sup> the real parts of the hadronic scattering amplitude,  $A_{\Re}(\mathbf{q}^2, \xi)$ , are given for a set of energies,  $\sqrt{s} = 1, 10, 10^2, \dots, 10^6 \text{ TeV}$ , as well as profile functions ( $T_{\Im}(b, \xi)$  and  $T_{\Re}(b, \xi)$ ) and  $K$ -matrix functions ( $K_{\Im}(b, \xi)$  and  $K_{\Re}(b, \xi)$ ).

In the present paper, on the basis of results of ref.,<sup>12,13</sup> we consider a combined action of the Coulomb and hadronic interactions for the diffractive scattering region. If the eikonal approach works, the straightforward way to take into account the interplay of these interactions is the use of the  $K$ -matrix function technique. We present the corresponding formulae (Section 2), results of numerical calculations for LHC energy (Section 3) and predictions for the larger energies in the case of the black disk mode for asymptotic regime (Section 4).

## 2. Diffractive scattering amplitude at ultrahigh energy and Coulomb interaction

The interplay of hadronic and Coulomb interactions was studied in a set of papers, see<sup>14-20</sup> and references therein. For ultrahigh energies and small  $\mathbf{q}^2$ , where the eikonal works, we present the  $K$ -matrix function technique which allow directly to take account the combined action of hadronic and Coulomb interactions ( $H + C$ ). The corresponding calculations of  $K^{H+C}(b, \xi)$  and the profile function  $T^{H+C}(b, \xi)$  are demonstrated.

### 2.1. Interplay of hadronic and Coulomb interactions in the $K$ -matrix function technique

We consider two types of scattering amplitudes and corresponding profile functions: the amplitude with combined interaction taken into account,  $A^{C+H}(\mathbf{q}^2, \xi)$

and  $T^{C+H}(b, \xi)$ , and that with the switched-off Coulomb interaction,  $A(\mathbf{q}^2, \xi)$  and  $T(b, \xi)$ .

For the combined interaction profile function we write:

$$T^{C+H}(b, \xi) = \frac{-2iK^{C+H}(b, \xi)}{1 - iK^{C+H}(b, \xi)} = \frac{-2i(K^C(b) + K(b, \xi))}{1 - i(K^C(b) + K(b, \xi))}, \quad (5)$$

where the Coulomb interaction is written as:

$$A^C(\mathbf{q}^2) = \pm i f_1(\mathbf{q}^2) \frac{4\pi\alpha}{\mathbf{q}^2 + \lambda^2} f_2(\mathbf{q}^2),$$

$$-2iK^C(b) = \pm i \int \frac{d^2q}{(2\pi)^2} e^{i\mathbf{q}\mathbf{b}} f_1(\mathbf{q}^2) \frac{4\pi\alpha}{\mathbf{q}^2 + \lambda^2} f_2(\mathbf{q}^2). \quad (6)$$

Here  $\alpha = 1/137$ ; the upper/lower signs refer to the same/opposite charges of the colliding particles. The cutting parameter  $\lambda$ , which removes the infrared divergency, can tend to zero in the final result for  $A^{C+H}(\mathbf{q}^2, \xi)$ . Colliding hadron form factors,  $f_1(\mathbf{q}^2)$  and  $f_2(\mathbf{q}^2)$ , guarantee the convergence of the integrals at  $\mathbf{q}^2 \rightarrow \infty$ ; for the  $pp^\pm$  collisions we use:

$$f_1(\mathbf{q}^2) = f_2(\mathbf{q}^2) = \frac{1}{(1 + \frac{\mathbf{q}^2}{0.71 \text{ GeV}^2})^2}. \quad (7)$$

The point which should be emphasized, the Eq. (5) gives us the amplitude imposed by the unitarity condition.

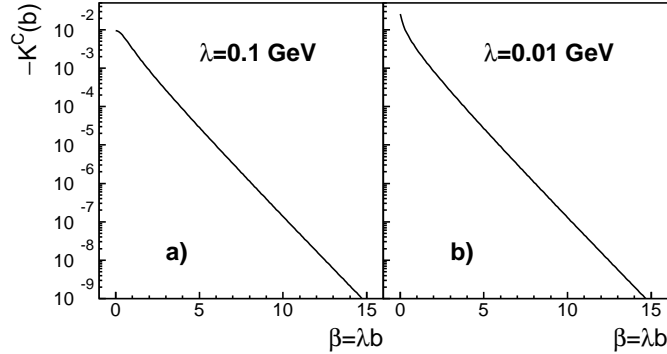


Fig. 1. The  $K$ -matrix function,  $-K^C(b)$ , for the pure Coulomb interaction in  $pp$  collision at different  $\lambda$  (a)  $\lambda = 0.1 \text{ GeV}$ , b)  $\lambda = 0.01 \text{ GeV}$ : we use  $\beta = \lambda b$  for abscissa.

### 3. Diffractive scattering cross section at the LHC energy and interference of hadronic and Coulomb interactions

On Fig. 1 we show  $-K^C(b)$  for  $\lambda = 0.1 \text{ GeV}$  (a) and  $0.01 \text{ GeV}$  (b). With these  $\lambda$ 's we calculate at  $\sqrt{s} = 7 \text{ TeV}$  the profile function  $T^{C+H}(b, \xi_{LHC})$  and the corresponding amplitude  $A^{C+H}(\mathbf{q}^2, \xi_{LHC})$ . Determination of the hadronic amplitude,

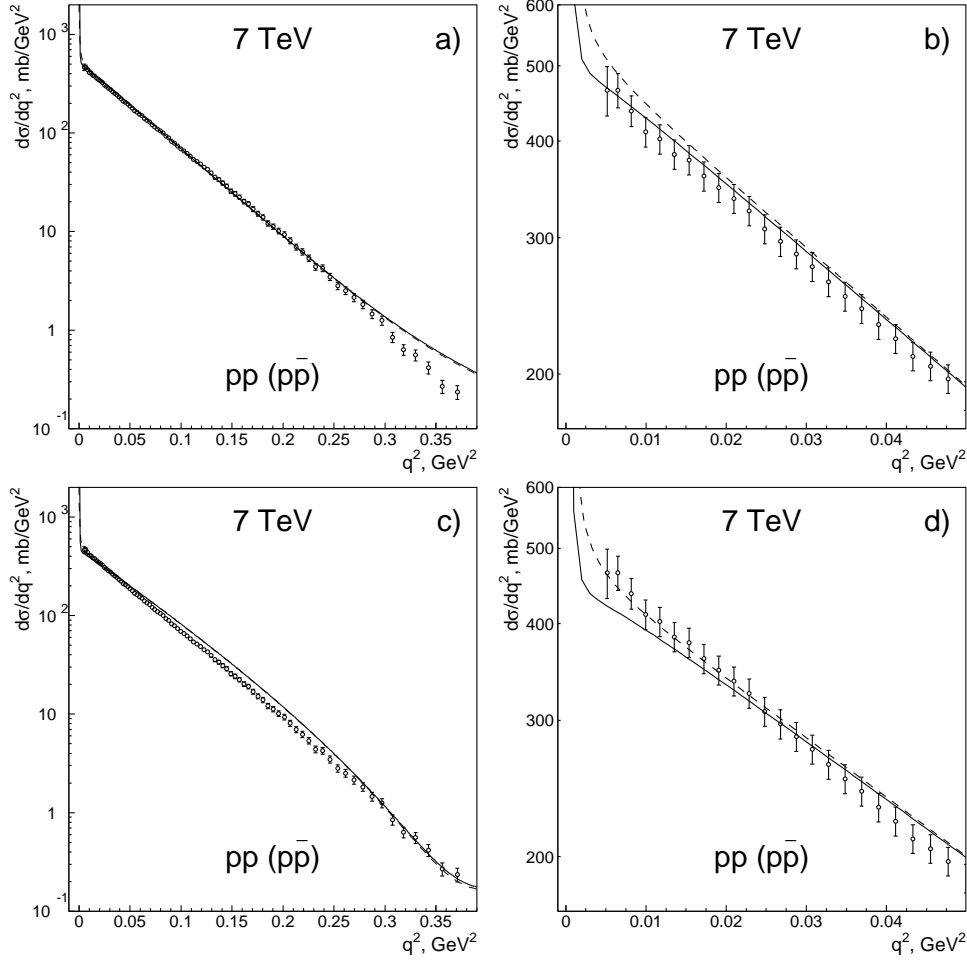


Fig. 2. Diffractive scattering cross section for  $pp$  at 7 TeV (TOTEM<sup>1</sup>) versus description with interplay of hadronic and Coulomb interactions ( $\lambda=0.01$  GeV): figures (a,b) refer to version (1) for determination of the hadronic amplitude, figures (c,d) to version (2); solid curves refer to  $pp$ , dashed ones to  $p\bar{p}$ .

$A_3(\mathbf{q}^2, \xi_{LHC})$ , is performed in terms of two versions:

- 1) with a direct application of the approximation (4) to the TOTEM data,<sup>1</sup>
- 2) Using the the results of the Dakhno-Nikonov model.<sup>9,10</sup>

The description of the data for  $\frac{d\sigma_{el}(\mathbf{q}^2, \xi_{LHC})}{dq^2}$  in terms of these two versions is shown in Fig. 2: here Figs. 2a,b refer to the version (1) and Figs. 2c,d correspond to version (2). Let us emphasise that the real part of the hadronic amplitude, given by Eq. (2), is taken here into account.

The Dakhno-Nikonov model gives a somewhat worse description of the  $\frac{d\sigma_{el}(\mathbf{q}^2, \xi_{LHC})}{dq^2}$  at 7 TeV than that using Eq. (4). This is not surprising because the

model describes the data in a broad energy interval, 0.5-50 TeV,<sup>10</sup> and the model parameters are responsible for the complete set of the data.

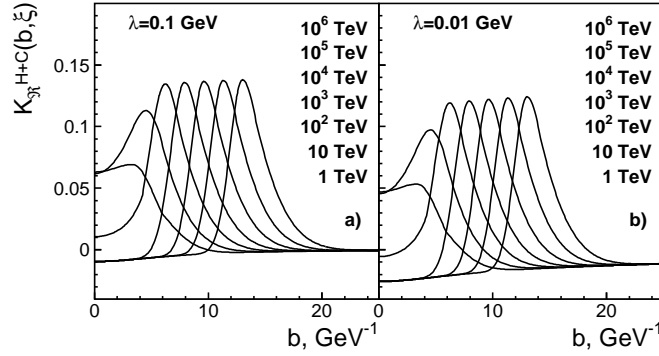


Fig. 3. Combined hadronic and Coulomb interactions for the  $pp$  scattering: Real parts of the  $K$ -matrix functions at different  $\lambda$  (a)  $\lambda = 0.1$  GeV, b)  $\lambda = 0.01$  GeV) at a set of energies  $\sqrt{s} = 1, 10, 10^2, \dots, 10^6$  TeV; at  $\sqrt{s} \geq 10^2$  TeV the black disk mode is supposed.

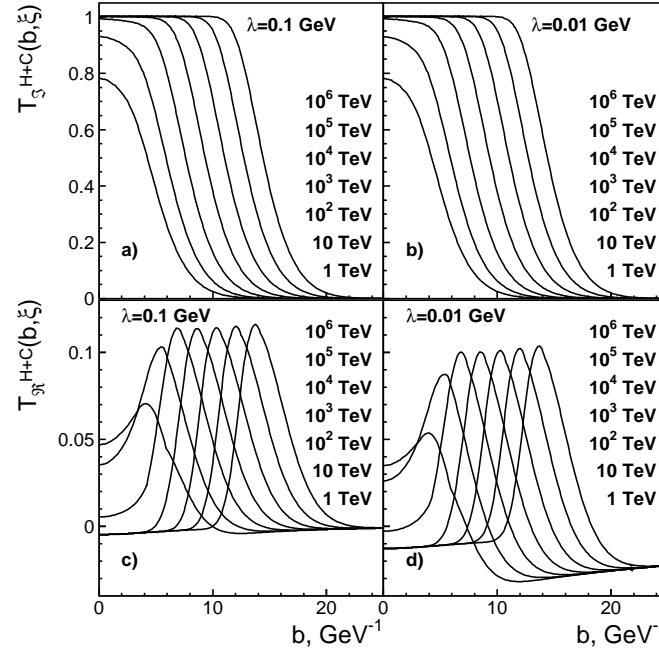


Fig. 4. Combined hadronic and Coulomb interactions for the  $pp$  scattering: Imaginary (a,b) and real parts (c,d) of the profile function at different  $\lambda$  (a,c)  $\lambda = 0.1$  GeV, b,d)  $\lambda = 0.01$  GeV) for a set of energies  $\sqrt{s} = 1, 10, 10^2, \dots, 10^6$  TeV; at  $\sqrt{s} \geq 10^2$  TeV the black disk mode is supposed.

#### 4. Black disk mode: predictions for ultrahigh energies

The inclusion of the Coulomb interaction into consideration of hadron diffractive scattering does not change the imaginary part of the  $K$ -matrix function,  $K_{\Im}^{H+C}(b, \xi) = K_{\Im}(b, \xi)$ . The real part of the  $K$ -matrix function for  $pp$  scattering,  $K_{\Re}^{H+C}(b, \xi) = K_{\Re}(b, \xi) + K^C(b)$ , is shown in Fig. 3 for  $b < 25 \text{ GeV}^{-1}$ .

Imaginary and real parts of the profile functions,  $T^{H+C}(b, \xi)$  for  $b < 25 \text{ GeV}^{-1}$ , are shown in Fig. 4; the inclusion of the Coulomb interaction leads to considerable perturbations in the real part, Figs. 4c,d.

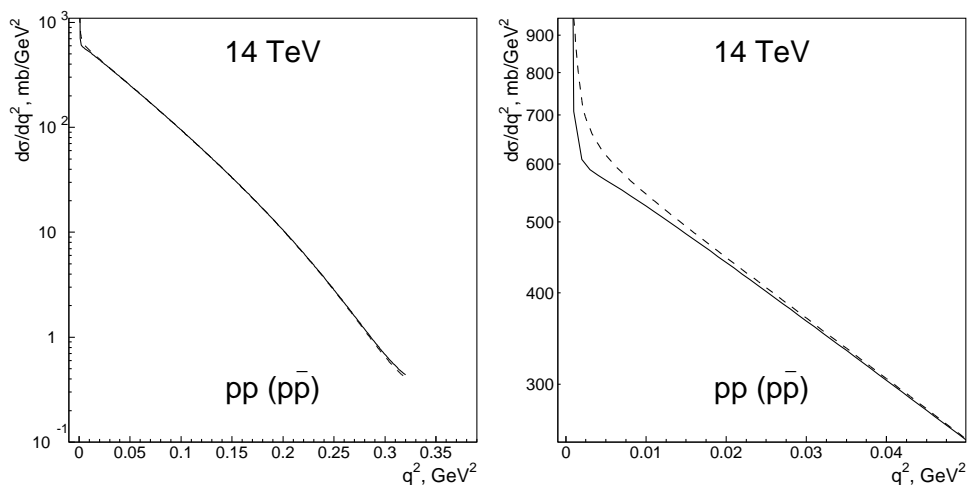


Fig. 5. Diffractive scattering cross sections for  $pp^{\pm}$  at 14 TeV. The real part of the hadronic amplitude as well as the interplay of the Coulomb and hadronic interactions are taken into account ( $\lambda=0.01 \text{ GeV}$ ): the solid curves refer to  $pp$ , dashed ones to  $p\bar{p}$ .

The predicted diffractive scattering cross sections  $\frac{d\sigma_{el}(q^2)}{dq^2}$  for  $pp^{\pm}$  at 14 TeV are shown in Fig. 5. Recall that we take into account here the real part of the hadronic amplitude as well as the interplay of the Coulomb and hadronic interactions.

#### 5. Conclusion

The interplay of the hadronic and Coulomb interactions at very small  $\mathbf{q}_{\perp}^2$  is discussed in terms of the  $K$ -matrix function. A specificity of the scattering amplitude at ultrahigh energy is dominance of the mass-on-shell contributions in intermediate rescattering states that results in the mass-on-shell origin of the  $K$ -matrix functions. Such  $K$ -matrix functions allow to incorporate the Coulomb interaction terms into the scattering amplitude straightforwardly by using a determination consistent with unitarity condition,  $K^C(b) = \tan \delta^C(s, b)$ . We present the corresponding formulae and perform calculations of  $\frac{d\sigma_{el}(q^2)}{dq^2}$  for  $pp^{\pm}$  at 7 TeV (Fig. 2) and 14 TeV (Fig. 5).

For ultrahigh energies we calculate  $K^{H+C}(b, \xi)$  and  $T^{H+C}(b, \xi)$  supposing the

black disk mode. However, the asymptotic high energy regime for diffractive hadron scatterings is not determined yet and the resonant disk regime<sup>21–23</sup> is not excluded at  $\sqrt{s} > 10^2$  TeV. Therefore an immediate task is to study the interplay of the Coulomb and hadronic interactions in the resonant disk mode.

### *Acknowledgment*

We thank Y.I. Azimov, J. Nyiri and A.V. Sarantsev for useful discussions. The work was supported by the Russian Science Foundation grant.

### **References**

1. G. Latino [on behalf of TOTEM Collaboration], EPJ Web Conf. **49**, 02005 (2013).
2. G. Aad *et al.* [ATLAS Collaboration], Eur. Phys. J. C **72**, 1926 (2012).
3. V. Khachatryan *et al.* [CMS Collaboration], Phys. Rev. D **92**, 012003 (2015).
4. B. Abelev *et al.* [ALICE Collaboration], Eur. Phys. J. C **73**, 6, 2456 (2013).
5. M. Froissart, Phys. Rev. **123**, 1053 (1961).
6. T. K. Gaisser and T. Stanev, Phys. Lett. B **219**, 375 (1989).
7. M. M. Block, F. Halzen and B. Margolis, Phys. Lett. B **252**, 481 (1990).
8. R. S. Fletcher, Phys. Rev. D **46**, 187 (1992).
9. L. G. Dakhno and V. A. Nikonov, Eur. Phys. J. A **5**, 209 (1999).
10. V. V. Anisovich, K. V. Nikonov and V. A. Nikonov, Phys. Rev. D **88**, 014039 (2013).
11. V. V. Anisovich, V. A. Nikonov and J. Nyiri, Phys. Rev. D **88**, 094015 (2013).
12. V. V. Anisovich, V. A. Nikonov and J. Nyiri, Int. J. Mod. Phys. A **30**, 1550188 (2015).
13. V. V. Anisovich, V. A. Nikonov and J. Nyiri, arXiv:1508.02140 [hep-ph].
14. H. A. Bethe, Annals Phys. **3**, 190 (1958).
15. L.D. Soloviev, Zh. Exp. Theor. Fiz. **49**, 292 (1966) [Sov. Phys. JETP **22**, 205 (1966)].
16. G. B. West and D. R. Yennie, Phys. Rev. **172**, 1413 (1968).
17. V. Franco, Phys. Rev. D **7**, 215 (1973).
18. R. Cahn, Z. Phys. C **15**, 253 (1982).
19. V. Kundrať and M. Lokajicek, Z. Phys. C **63**, 619 (1994).
20. J. Kaspar, V. Kundrať, M. Lokajicek and J. Prochazka, Nucl. Phys. B **843**, 84 (2011).
21. S. M. Troshin and N. E. Tyurin, Int. J. Mod. Phys. A **29**, 1450151 (2014).
22. I. M. Dremin, Bull. Lebedev Phys. Inst. **42**, 21 (2015) [Kratk. Soobshch. Fiz. **42**, 8 (2015)].
23. V. V. Anisovich, V. A. Nikonov and J. Nyiri, Phys. Rev. D **90**, 074005 (2014).